

Anticancer activity, DNA binding and docking study of M(II)-complexes (M=Zn, Cu and Ni) derived from a new pyrazine-thiazole ligand: Synthesis, structure and DFT

Pradip Bera^{a,d}, Abhishek Aher^b, Paula Brandao^c, Sunil K Manna^{*b}, Indranil Bhattacharyya^a, Gopinath Mondal^a, Abhimanyu Jana^a, Ananyakumari Santra^a and PulakeshBera^{*a}

Table S1: Crystal parameters of **PyztbH**, **1**, **2**, **3** and **4**

Table S2: Selected bond angle of the **PyztbH** and **1**, **2**, **3** and **4**

Table S3: Hydrogen bond parameters (Å) for **PyztbH** and **2**

Figure S1. UV-Vis spectra of the **PyztbH**, **1**, **2**, **3** and **4** at 10^{-5} M in MeOH solution.

Figure S2. Fluorescence emission plot of **PyztbH**, **1**, **2**, **3** and **4** in DMSO solvent at 10^{-5} M ($\lambda_{\text{ex}} = 330$ nm).

Figure S3. π - π stacking interaction and 1D hydrogen bonded supramolecular chain along a-axis of **PyztbH**

Figure S4. π - π stacking interaction of **1**

Figure S5. 3D hydrogen bonded supramolecular Structure and molecular association along the b-axis of **2**

Figure S6. π - π stacking interaction of **3**

Figure S7. π - π stacking interaction of **4**

Figure S8. a) Capped-ball and stick model viewed into groove binder of DNA with **1**. The important interactions between different sections of the **1**-DNA complex are illustrated with green, red and gray solid line. The non-coordinate acetyl -CH₃ group, benzene ring interacts with DNA by hydrophobic and $\pi_{\text{adinine}}-\pi$ stacking interaction respectively (b) space filled model of binding mode and hydrophobic interaction of **1** with DNA.

Figure S9. a) Capped-ball and stick model viewed into groove binder of DNA with **2**. The important interactions between different sections of the **2**-DNA complex are illustrated with dotted solid line. (b) space filled model of binding mode and hydrophobic interaction of **2** with DNA.

Figure S10. a) Capped-ball and stick model viewed into intercalate binder of DNA with **4**. The important interactions between different sections of the **4**-DNA complex are illustrated

with arrow solid line. (b) Space filled model of binding mode and hydrophobic interaction of **4** with DNA.

Figure S11. Effect of compounds on cytotoxicity of different cancer cells.

Table S1: Crystal parameters of **PyztbH**, **1**, **2**, **3** and **4**

Parameter	PyztbH	1	2	3	4
CCDC/CSD	1865480	1960775	1960776	1960777	1960778
Empirical formula	C ₁₆ H ₁₂ N ₆ S	C ₃₂ H ₂₂ N ₁₂ S ₂ Zn	C ₁₉ H ₁₄ N ₈ S ₃ ZnO ₂ , 2(C ₁₆ H ₁₂ N ₆ S)	C ₁₇ H ₁₅ CuN ₉ OS	C ₃₂ H ₂₂ N ₁₂ NiS ₂ ClO ₄
Fw, g/M	320.38	704.13	1188.70	456.99	796.88
Crystal system	Monoclinic	monoclinic	Monoclinic	Triclinic	Triclinic
Space group	P21/n	C2/c	C2/c	P $\bar{1}$	P $\bar{1}$
a (Å)	7.9257(6)	37.6726(13)	36.253(2)	7.0292(5)	9.7741(11)
b (Å)	17.9072(12)	9.0541(3)	14.2625(8)	11.1309(9)	12.1509(13)
c (Å)	10.7961(7)	18.5487(7)	25.1293(14)	12.1913(9)	14.0740(16)
A	90	90	90	77.463(3)	94.392(4)
B	92.024(2)	105.77	125.447(1)	87.811(3)	90.811(4)
Γ	90	90	90	81.426(3)	94.002(4)
V (Å ³)	1531.30(18)	6088.6(4)	10585.0(10)	920.70(12)	1662.2(3)
Z	4	1.536	8	2	2
T(k)	150	150	150	150	150
σ calcd, g cm ⁻³	1.390	1.536	1.492	1.648	1.592
μ (mm ⁻¹)	0.220	0.991	0.725	1.331	0.849
F (000)	664	2880	4880	466	814
R, wR, S	0.0385, 0.1018, 1.04	0.0347, 0.0841, 1.04	0.0546, 0.1405, 1.03	0.0346, 0.0817, 1.04	0.0487, 0.1315, 1.03

Table S2: Selected bond angle of the **PyztbH** and **1**, **2**, **3** and **4**

PyztbH		1		2		3		4	
Bond	Angle(°)	Bond	Angle (°) Crystal DFT	Bond	Angle (°) Crystal DFT	Bond	Angle (°) Crystal DFT	Bond	Angle (°) Crystal DFT
N1-C4-C5	118.04(12) 117.84	N1-Zn-N3	74.46(7) 74.43	N1-Zn-N3	73.26(15) 73.30	N1-Cu-N3	79.10(7) 78.66	N1-Ni-N3	82.20(11) 82.19
C5-N3-N4	119.74(11) 119.65	N1-Zn-N7	88.38(7) 88.44	N1-Zn-N7	95.99(13) 95.96	N1-Cu-N5	158.57(7) 157.69	N1-Ni-N7	91.67(10) 91.67
N4-C7-N5	123.41(12) 123.38	N1-Zn-N9	95.72(8) 95.75	N1-Zn-N8	94.05(15) 93.99	N1-Cu-N7	91.79(7) 91.77	N1-Ni-N9	94.22(11) 94.25
N5-C9-C10	118.15(11) 118.10	N1-Zn-N11	93.17(7) 93.13	N3-Zn-N5	76.58(14) 76.58	N3-Cu-N5	79.47(7) 79.05	N1-Ni-N11	88.98(10) 88.98
C3-C4-C5	120.89(11) 120.64	N3-Zn-N5	76.82(8) 76.71	N3-Zn-N7	118.64(15) 118.52	N3-Cu-N7	164.38(8) 164.07	N3-Ni-N5	81.43(10) 81.37
		N3-Zn-N7	90.08(7) 90.12	N3-Zn-N8	132.54(16) 132.41	N1-Cu-O1	89.19(6) 89.84	N3-Ni-N7	93.20(10) 93.23
		N3-Zn-N9	161.70(8) 161.71	N7-Zn-N5	101.77(14) 11.74	N3-Cu-O1	93.63(6) 94.03	N3-Ni-N9	174.53(11) 174.56
		N3-Zn-N11	117.75(8) 117.82	N7-Zn-N8	107.91(15) 108.16	N5-Cu-O1	92.45(6) 92.53	N3-Ni-N11	102.53(10) 102.51
		N5-Zn-N7	89.76(7) 89.73	N8-Zn-N5	103.54(15) 103.52	N7-Cu-O1	98.95(7) 98.70	N5-Ni-N7	90.18(10) 90.19
		N5-Zn-N9	111.34(7)					N5-Ni-N9	102.18(10)

			111.43						102.21
		N5–Zn–N11	101.88(7) 102.01					N5–Ni–N11	93.64(11) 93.65
		N7–Zn–N9	73.99(7) 73.97					N7–Ni–N9	82.74(10) 82.73
		N7–Zn–N11	151.50(8) 151.38					N7–Ni–N11	164.19(9) 164.18
		N9–Zn–N11	77.54(8) 77.45					N9–Ni–N11	81.46(10) 81.46

Table S3: Hydrogen bond parameters (Å) for **PyztbH** and **2**

Compound	D–H ...A	D–H (Å)	H...A (Å)	D...A (Å)	D–H...A (°)	Symmetry operation on A
PyztbH	N4 H4 N2	0.873(18)	2.095(18)	2.9515(17)	166.9(15)	$-1/2+x, 3/2-y, 1/2+z$
2	N4 H4 O200	0.89(5)	1.86(5)	2.716(7)	162(4)	$-1/2+x, -1/2+y, z$
	N12 H12A O100	0.90(5)	2.27(5)	3.113(7)	157(4)	
	N18 H18A N6	0.91(5)	2.20(5)	2.20(5)	165(4)	
	O200 H20A N14	0.82(5)	2.08(4)	2.889(6)	169(6)	
	O200 H20B O100	0.84(6)	1.96(5)	2.792(6)	173(6)	

FIGURES

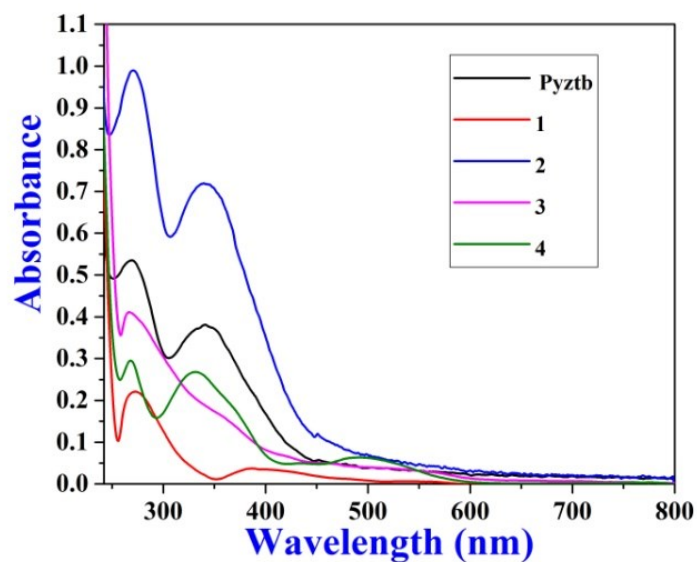


Figure S1. UV-Vis spectra of the **PyztbH**, **1**, **2**, **3** and **4** at 10^{-5} M in DMSO.

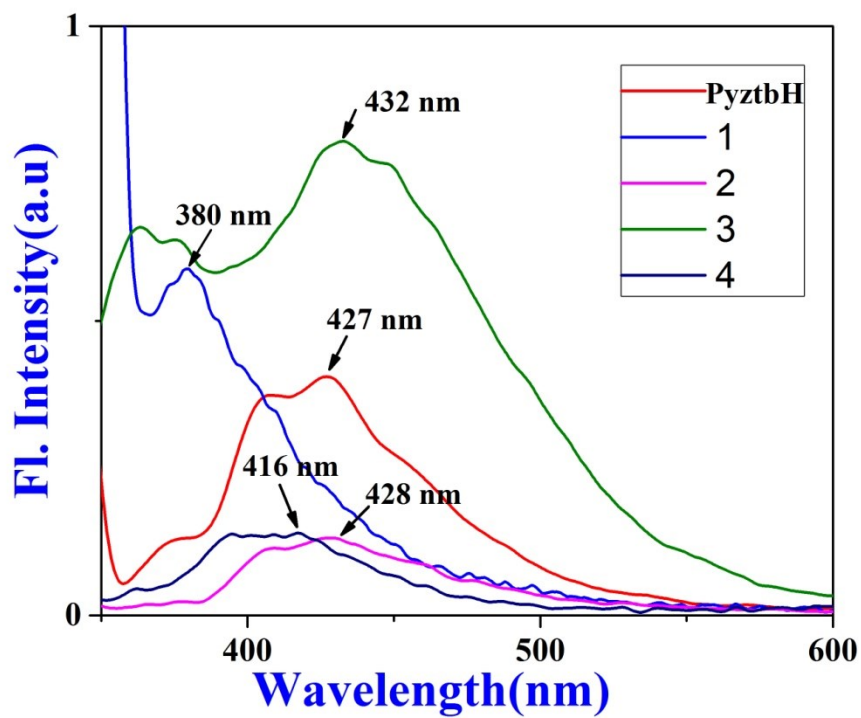


Figure S2. Fluorescence emission plot of PzbtbH, 1, 2, 3 and 4 in DMSO at 10^{-5} M ($\lambda_{\text{ex}} = 330$ nm).

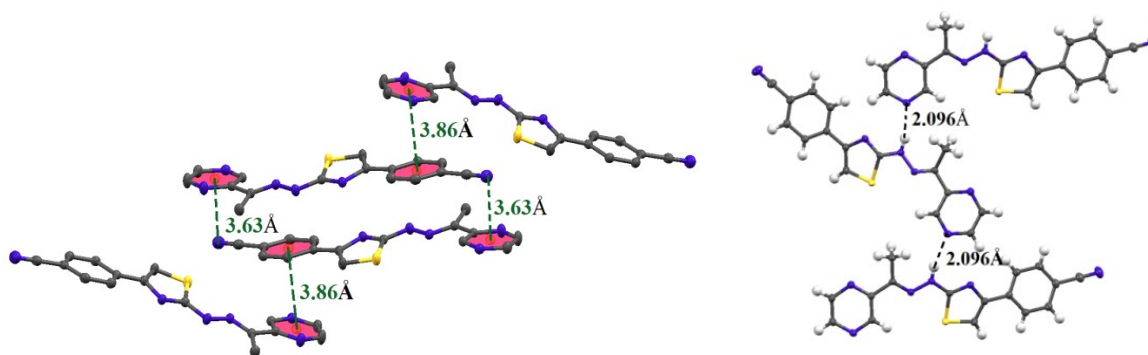


Figure S3. π - π stacking interaction and 1D hydrogen bonded supramolecular chain along a-axis of PzbtbH

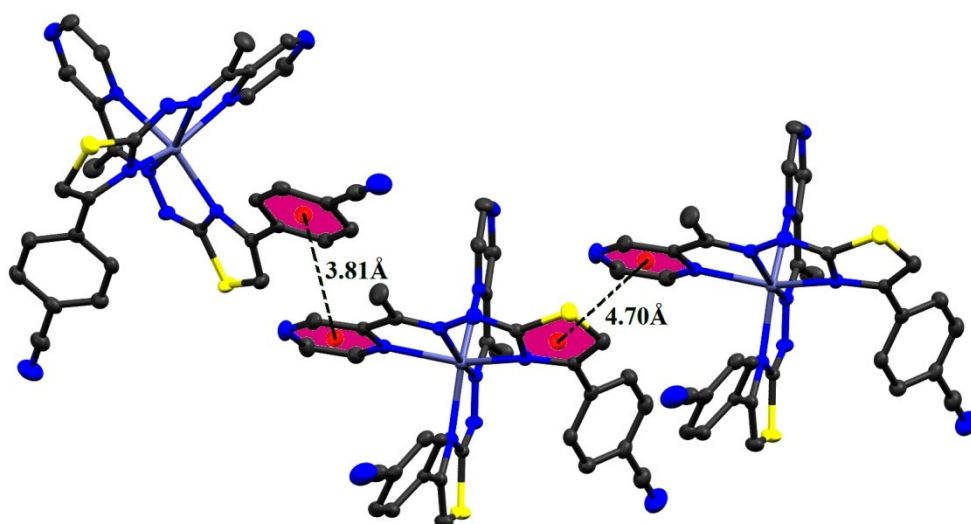


Figure S4. π - π stacking interaction of **1**.

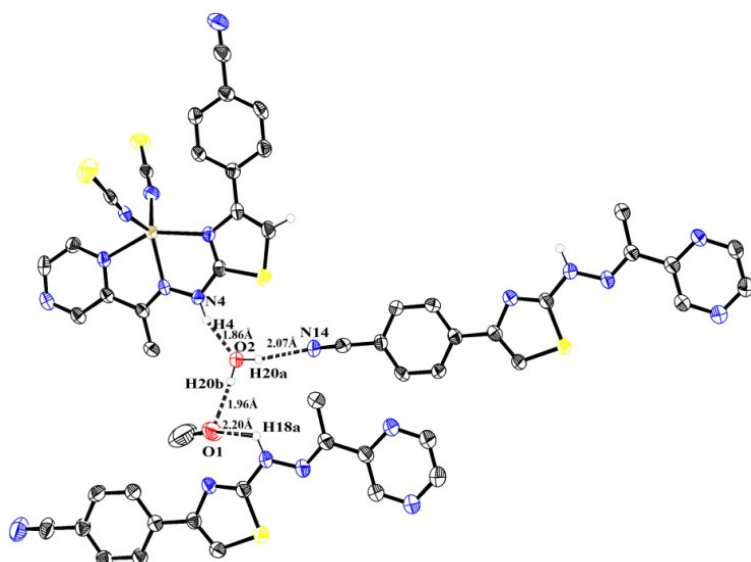


Figure S5. 3D hydrogen bonded supramolecular structure and molecular association along the b-axis of **2**.

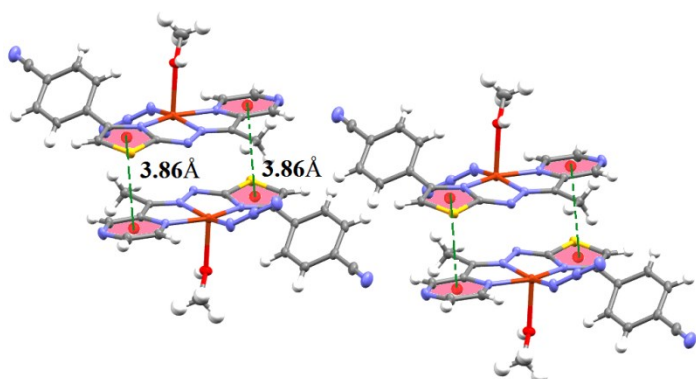


Figure S6. π - π stacking interaction in **3**

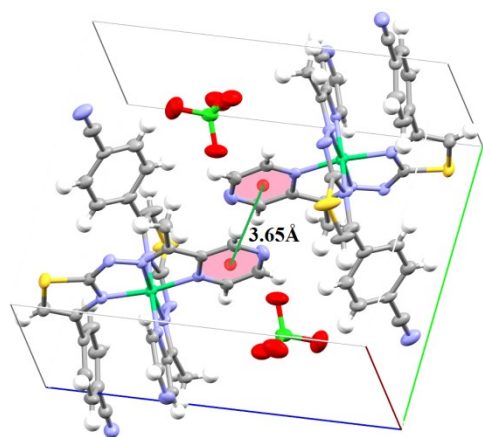


Figure S7. π - π stacking interaction in **4**

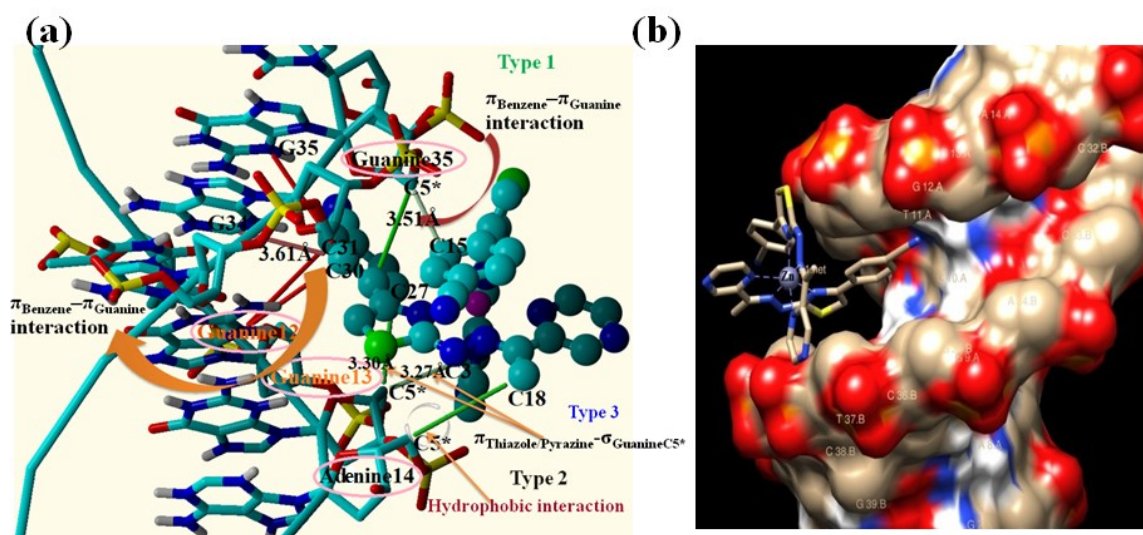


Figure S8. a) Capped-ball and stick model viewed into groove binder of DNA with **1**. The important interactions between different sections of the **1**-DNA complex are illustrated with green, red and gray solid line. The non-coordinate acetyl -CH₃ group, benzene ring interacts with DNA by hydrophobic and $\pi_{\text{adimine}}-\pi$ stacking interaction respectively (b) space filled model of binding mode and hydrophobic interaction of **1** with DNA.

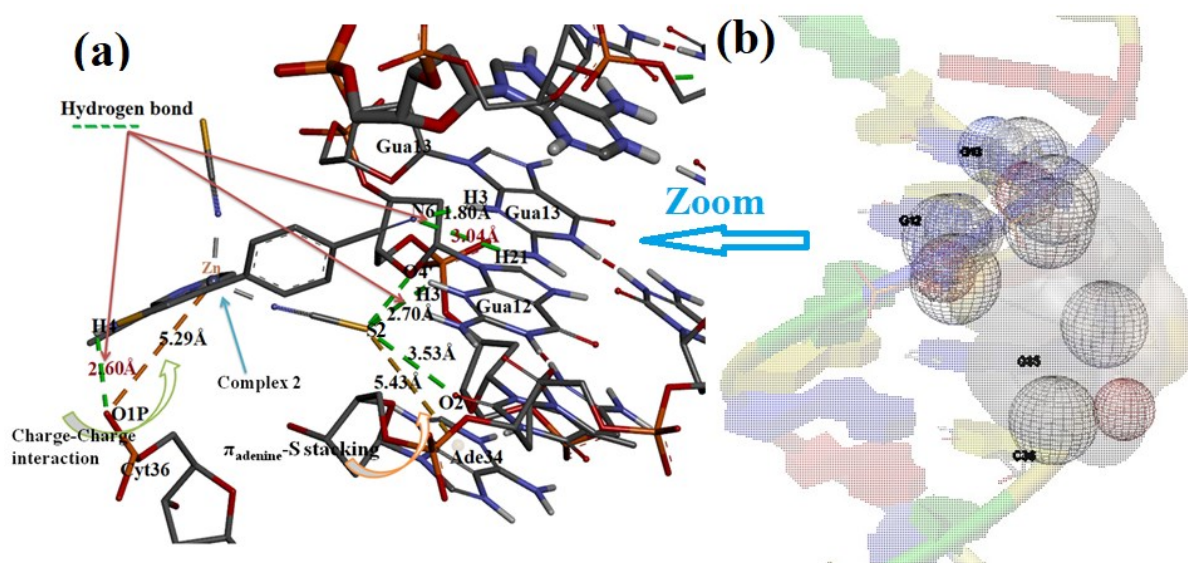


Figure S9. a) Capped-ball and stick model viewed into groove binder of DNA with **2**. The important interactions between different sections of the **2**-DNA complex are illustrated with dotted solid line. (b) space filled model of binding mode and hydrophobic interaction of **2** with DNA.

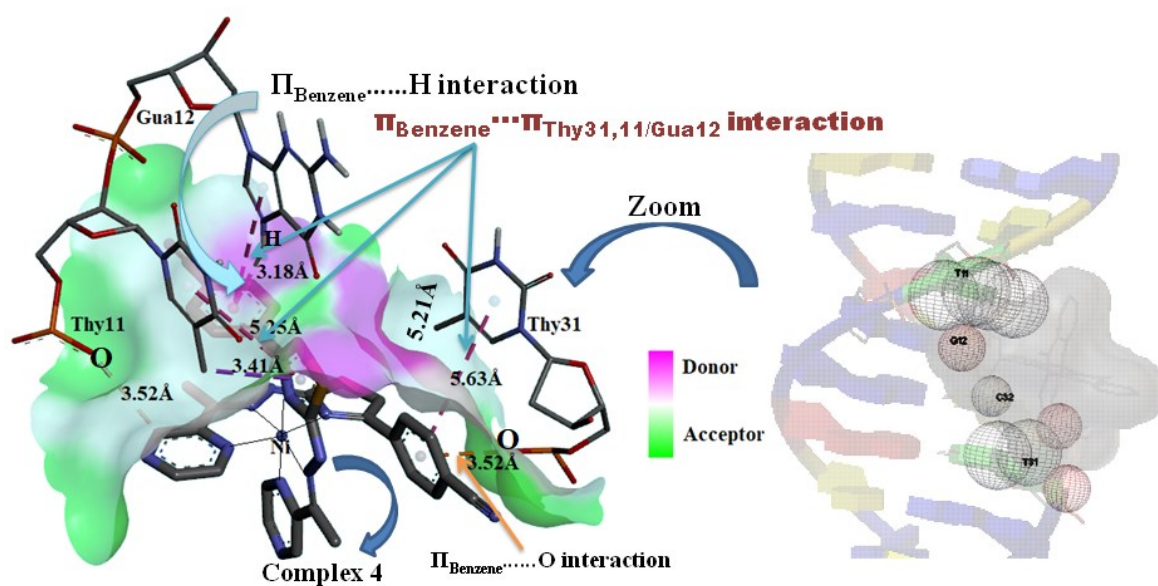


Figure S10. a) Capped-ball and stick model viewed into intercalate binder of DNA with **4**. The important interactions between different sections of the **4**-DNA complex are illustrated with arrow solid line. (b) Space filled model of binding mode and hydrophobic interaction of **4** with DNA.

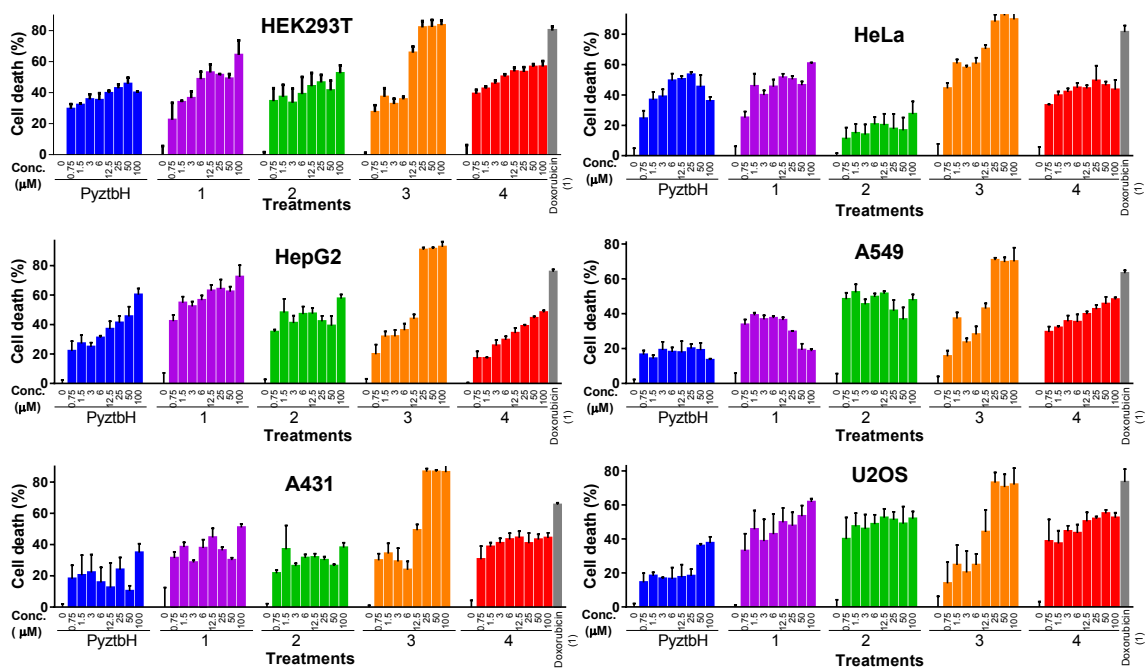


Figure S11. Effect of compounds on cytotoxicity of different cancer cells. Several tumor cells (5000 cell/well of 96-Well plate) were treated with different concentrations of ligand (PyztbH) and its derivatives **1**, **2**, **3** and **4** for 72 h in triplicate. MTT cell viability was assayed. Doxorubicin (1 μM) treated cells was considered as positive control. Mean cell death from triplicate samples were calculated in percentage, considering untreated cell death is 0% and indicated in the graph. Data were transformed, normalized and IC_{50} values were calculated using Graph Pad Prism.

